On inverse doping profile problems for the voltage-current map

A. Leitão[1] P.A. Markowich[2] J.P. Zubelli[3]

November 2, 2005

[1] Department of Mathematics, Federal University of St. Catarina, P.O. Box 476, 88040-900 Florianopolis, Brazil (aleitao@mtm.ufsc.br)
[2] Department of Mathematics, University of Vienna, Boltzmanngasse 9, A-1090 Vienna, Austria (peter.markowich@univie.ac.at)
[3] IMPA, Est. D. Castorina 110, 22460-320 Rio de Janeiro, Brazil (zubelli@impa.br)

Abstract

We consider the problem of identifying possibly discontinuous doping profiles in semiconductor devices from data obtained by stationary voltage-current maps. In particular we focus on the so-called *unipolar case*, a system of PDE's derived directly from the drift diffusion equations. The related inverse problem corresponds to an inverse conductivity problem with partial data. Two distinct approaches for solving the identification problem are presented: a Landweber-Kaczmarz method and a level set type method. Numerical implementations of both methods show the different effectiveness of these approaches.

1 Introduction

The starting point of the mathematical model discussed in this paper is the system of *stationary drift diffusion equations* (see system (8) in Section 2). This system of equations, derived more than fifty year ago [28], is the most widely used to describe semiconductor devices and represents an accurate compromise between efficient numerical solvability of the mathematical model and realistic description of the underlying physics [22, 23, 26].

This paper is devoted to the analysis of an identification problem related to a particular model, the so called *unipolar system*, derived from the stationary drift diffusion equations under certain simplifying assumptions on the concentration of free carriers of positive charges and on the recombination-generation rate. In this framework, the parameter function to be identified is the *doping profile* (a parameter function in a system of PDE's). This parameter depends on the space variables only and represents the doping concentration, which gives the performance of the device. It is produced by diffusion of different materials into the silicon crystal and by implantation with an ion beam.

In practical experiments there are different types of measurement techniques, such as *Laser-Beam-Induced Current* (LBIC) measurements, *Capacitance* measurements, *Current Flow* measurements (refer to [11, 12, 13] for the first type and to [4, 5, 6] for the others). These measurement techniques are related to different

types of data and lead to different inverse problems for reconstructing the doping profile. They are the so-called *inverse doping profile problems*. We shall focus on reconstruction problems based on data generated by the *voltage-current* (V-C) map, i.e., an operator that takes the applied voltage at a specified boundary part (corresponding to a semiconductor contact) into the outflow current density on a different boundary part (another contact). The two main contributions of this paper consists of a theoretical identification result for a discretized version and the analysis of a numerical method (a level set type method) for solving the inverse doping profile problem in the unipolar case.

The precise implantation of the doping profile is crucial for the desired performance of the semiconductor device. As far as applications are concerned, there is substantial interest in replacing expensive laboratory testing by numerical simulation and non-destructive testing, in order to minimize manufacturing costs of semiconductors as well as for quality control. Therefore, the development, as well as the analysis, of efficient algorithms for inverse doping profile problems are perfectly justified from a practical viewpoint.

This paper is organized as follows: In Section 2 we briefly introduce the *drift diffusion* equations, formally define the V-C map, and derive the *unipolar system* (see system(11)). The latter models the direct problem related to the inverse doping profile problem analyzed in this paper.
In Section 3 we treat the identification issue for this inverse problem. We do not have, at present, a theoretical result showing uniqueness in the identification of the doping profile. However, we do present two lines of reasoning that support the conjecture of an identifiability result for the doping profile: The first one is based on recent results due to Bukhgeim and Uhlmann [3] on global uniqueness for the local Dirichlet-to-Neumann map; The second one concerns a discretized version of the problem that falls within the scope of tomography in the presence of diffusion and scattering [16, 17].
In Section 4 a Landweber-Kaczmarz iterative method is proposed to reconstruct the doping profile function. This corresponds to the simplest idea (a steepest descent method) for solving the least square formulation the inverse problem. A numerical implementation of the method is presented. The sensibility of the reconstruction with respect to the number of sources is investigated.
In Section 5 we use a level set type method to solve the identification problem. In this approach, a single pair of (voltage, current) data is used. Nevertheless, the quality of the reconstruction is much better than the one obtained by the Landweber-Kaczmarz method. An analytical result concerning stability, convergence and well-posedness of this level set method is also presented. Section 6 is devoted to final comments and conclusions.

2 Inverse doping profile problems

2.1 Drift diffusion equations

The *drift diffusion* equations are the most widely used model to describe semiconductor devices. The mathematical modeling of semiconductor equations has developed significantly, together with their manufacturing. The *basic semiconductor device equations* were first presented, in the level of completeness discussed here, by W.R. van Roosbroeck in [28]. Since then, it has been subject of intensive mathematical and numerical investigation. Recent detailed expositions of the subject of modeling, analysis and simulation of semiconductor equations can be found, e.g., in [22, 23, 26].

The stationary drift diffusion equations consist of the Poisson equation (1) for the electrostatic potential V and the continuity equations (2) and (3) for the electron density n and the hole density p respectively (notice that $-\nabla V$ is the electric field, while n and p are the concentration of free carriers of negative charge and positive charge respectively).

$$\begin{aligned} \mathrm{div}(\epsilon \nabla V) &= q(n - p - C) \text{ in } \Omega & (1)\\ \mathrm{div} J_n &= R \qquad\qquad \text{in } \Omega & (2)\\ \mathrm{div} J_p &= -R \qquad\qquad \text{in } \Omega, & (3) \end{aligned}$$

where $J_n = \mu_n(\nabla n - n\nabla V)$ and $J_p = -\mu_p(\nabla p + p\nabla V)$. A word on notation:

- The domain $\Omega \subset \mathbb{R}^d$ $(d = 2, 3)$ represents the semiconductor device;
- The positive constants ϵ and q denote the permittivity coefficient and the elementary charge respectively;
- μ_n and μ_p represent the mobilities of electrons and holes respectively;
- D_n and D_p are diffusion coefficients for electrons and holes respectively;
- $R = R(n, p, x)$ denotes the recombination-generation rate, which is typically a function of the type: $R = \mathcal{R}(n, p, x)(np - n_i^2)$, where n_i denotes the intrinsic charge density.
- The function $C = C(x)$ denotes the doping concentration, which is produced by diffusion of different materials into the silicon crystal and by implantation with an ion beam.

In many technological applications, the *doping profile* C is the parameter that has to be identified. After the manufacturing process of the semiconductor device, it is often necessary to test whether the doping has been correctly implanted. The inverse problem we are concerned with is related to a non destructive identification procedure, based on experiments modeled by the *voltage to current* operator (see Subsection 2.2).

In the sequel we discuss the corresponding boundary conditions for system (1)–(3). The boundary of Ω is assumed to be divided in two nonempty parts: $\partial\Omega = \partial\Omega_N \cup \partial\Omega_D$. On the Dirichlet part of the boundary, $\partial\Omega_D$, the following boundary conditions are prescribed:

$$\begin{aligned} V = V_D(x) &:= U(x) + V_{\mathrm{bi}}(x) && \text{on } \partial\Omega_{\mathrm{D}}, & (4)\\ n = n_D(x) &:= \tfrac{1}{2}\big(C(x) + \sqrt{C(x)^2 + 4n_i^2}\big) && \text{on } \partial\Omega_{\mathrm{D}}, & (5)\\ p = p_D(x) &:= \tfrac{1}{2}\big(-C(x) + \sqrt{C(x)^2 + 4n_i^2}\big) && \text{on } \partial\Omega_{\mathrm{D}}, & (6) \end{aligned}$$

where $U(x)$ is the applied potential, (differences in $U(x)$ between different segments of $\partial\Omega_D$ correspond to the applied bias between these two contacts), $V_{\mathrm{bi}}(x) := U_T \ln(n_D(x)/n_i)$ and the constant U_T denotes the thermal voltage.

The Neumann part of the boundary $\partial\Omega_N = \partial\Omega - \partial\Omega_D$ models insulating or artificial surfaces. Therefore, a zero current flow and a zero electric field in the normal direction are prescribed, i.e., homogeneous boundary conditions, in terms of the current densities[1] J_n and J_p, are supplied:

$$\nabla V \cdot \nu = J_n \cdot \nu = J_p \cdot \nu = 0 \text{ on } \partial\Omega_{\mathrm{N}}. \qquad (7)$$

[1] The densities of the electron and hole current J_n and J_p satisfy the current relations:

$$J_n = q(D_n \nabla n - \mu_n n \nabla V), \quad J_p = q(-D_p \nabla p - \mu_p p \nabla V), \quad \text{in } \Omega.$$

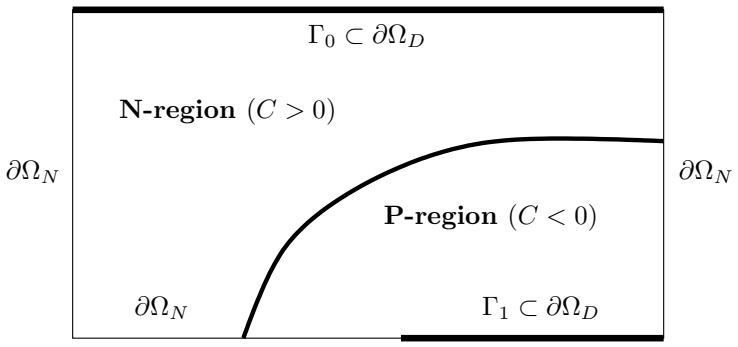

Figure 1: The domain $\Omega \subset \mathbb{R}^2$ represents a P-N diode. The P-region corresponds to the subregion of Ω, where $C < 0$. In the N-region $C > 0$ holds. The curve between these regions is called *p-n junction.*

Using an adequate change of variables (motivated by the Einstein relations: $D_n = U_T\mu_n$, $D_p = U_T\mu_p$), it is possible to rewrite system (1)–(7) in a more convenient way. Indeed, first we define the *Slotboom variables* (u, v) by

$$n(x) \;=\; n_i \exp(V(x)/U_T)\, u(x), \quad p(x) \;=\; n_i \exp(-V(x)/U_T)\, v(x)$$

and rescale both the potential and the mobilities: $V(x) := V(x)/U_T$, $\tilde{\mu}_n := qU_T\mu_n$, $\tilde{\mu}_p := qU_T\mu_p$. Then, we obtain the system

$$\begin{aligned}
\lambda^2 \Delta V &= \delta^2\big(e^V u - e^{-V} v\big) - C && \text{in } \Omega && (8a)\\
\operatorname{div} J_n &= \delta^4\, Q(V,u,v,x)\,(uv-1) && \text{in } \Omega && (8b)\\
\operatorname{div} J_p &= -\delta^4\, Q(V,u,v,x)\,(uv-1) && \text{in } \Omega && (8c)\\
V = V_D &:= U + V_{\mathrm{bi}} && \text{on } \partial\Omega_{\mathrm{D}} && (8d)\\
u = u_D &:= e^{-U} && \text{on } \partial\Omega_{\mathrm{D}} && (8e)\\
v = v_D &:= e^{U} && \text{on } \partial\Omega_{\mathrm{D}} && (8f)\\
\nabla V \cdot \nu = J_n \cdot \nu &= J_p \cdot \nu \;=\; 0 && \text{on } \partial\Omega_{\mathrm{N}} && (8g)
\end{aligned}$$

Two dimensionless positive parameters occur, namely ϵ and δ (see [22, 23] for the formulas), both small in many practical applications. Existence (in weak sense) and some uniqueness results for system (8) can be found in [22, 23]. One can prove, under suitable regularity assumptions on the boundary conditions u_D, v_D, U and on the doping profile C, that system (8) admits a weak solution (V, u, v) in $(H^1(\Omega)\cap L^\infty(\Omega))^3$ (we refer to [23, Theorem 3.3.16] and [5, Theorem 4.2]). Stronger existence results in $(H^2(\Omega) \cap L^\infty(\Omega))^3$ can be found in [22].

2.2 Derivation of the inverse problem

We start by defining the *voltage-current* (V-C) map:

$$\begin{aligned}
\Sigma_C : H^{3/2}(\partial\Omega_D) &\;\to\; L^2(\Gamma_1)\\
U &\;\mapsto\; J\cdot\nu|_{\Gamma_1} \;=\; (J_n + J_p)\cdot\nu|_{\Gamma_1}\,,
\end{aligned}$$

where $\Gamma_1 \subset \partial\Omega_D$ corresponds to the part of the boundary (a contact) where measurements are taken (an example of a very simple semiconductor device, a P-N diode, is shown in Figure 1). Since the potential can be shifted by a constant, we shall assume w.l.o.g. that $U_{\Gamma_1} = 0$. In practical applications, the function $U \in H^{3/2}(\partial\Omega_D)$ modeling the voltage input in (8) is assumed to be piecewise constant in the contacts.

In the sequel we review some properties of the operator Σ_C. A complete proof can be found in [5].

Lemma 2.1. *The current $\Sigma_C(U) \in L^2(\Gamma_1)$ is uniquely defined for each voltage $U \in H^{3/2}(\partial\Omega_D)$ in the neighborhood of $U \equiv 0$, i.e., the operator Σ_C is well-defined in the neighborhood of $U \equiv 0$. Moreover, Σ_C is continuous and continuously Fréchet differentiable in the neighborhood of $U \equiv 0$.*

The map Σ_C takes the applied voltage U into the corresponding current density. The linearized unipolar case (close to equilibrium) corresponds to the model obtained from the drift diffusion equations by linearizing the V-C map at $U = 0$. This simplification is motivated by the fact that, due to hysteresis effects for the large applied voltage, the V-C map is single valued only in a neighborhood of $U = 0$. The Gateaux derivative of Σ_C at $U = 0$ in direction $h \in H^{3/2}(\partial\Omega_D)$ is given by

$$\Sigma_C'(0)h = \left(\mu_n e^{V_{\rm bi}}\hat{u}_\nu - \mu_p e^{-V_{\rm bi}}\hat{v}_\nu\right)|_{\Gamma_1},$$

where $(\hat{u}, \hat{v})$ solve

$$\left\{\begin{array}{lll} \operatorname{div}(\mu_n e^{V^0}\nabla\hat{u}) = Q_0(V^0, x)(\hat{u}+\hat{v}) & \text{in } \Omega \\ \operatorname{div}(\mu_p e^{-V^0}\nabla\hat{v}) = Q_0(V^0, x)(\hat{u}+\hat{v}) & \text{in } \Omega \\ \hat{u} = -h \quad \text{and} \quad \hat{v} = h & \text{on } \partial\Omega_D \\ J_n\cdot\nu = J_p\cdot\nu = 0 & \text{on } \partial\Omega_N \end{array}\right. \tag{9}$$

and V^0 is a solution of the *Poisson equation at equilibrium*

$$\left\{\begin{array}{rcll} \lambda^2\Delta V^0 & = & e^{V^0} - e^{-V^0} - C & \text{in } \Omega \\ V^0 & = & V_{\rm bi} & \text{on } \partial\Omega_D \\ \nabla V^0\cdot\nu & = & 0 & \text{on } \partial\Omega_N\,. \end{array}\right. \tag{10}$$

From now on, the following simplifying assumptions are made:

A1) The concentration of holes satisfy $p = 0$ (or $v = 0$);

A2) No recombination-generation rate is present, i.e., $\mathcal{R} = 0$ (or $Q = 0$);

A3) The electron mobility is constant, i.e., $\mu_n = 1$.

Under those assumptions, the decoupled system (9)-(10) reduces to:

$$\left\{\begin{array}{ll} \lambda^2\Delta V^0 = e^{V^0} - C & \text{in } \Omega \\ V^0 = V_{\rm bi} & \text{on } \partial\Omega_D \\ \nabla V^0\cdot\nu = 0 & \text{on } \partial\Omega_N \end{array}\right. \qquad \left\{\begin{array}{ll} \operatorname{div}(e^{V^0}\nabla u) = 0 & \text{in } \Omega \\ u = U & \text{on } \partial\Omega_D \\ J_n\cdot\nu = 0 & \text{on } \partial\Omega_N \end{array}\right. \tag{11}$$

(notice that we skipped the '$\hat{}$' in the above notation).

The inverse problem of identifying the doping profile in the linearized unipolar model (11) corresponds to the identification of $C(x)$ from the map

$$\begin{array}{rccl} F: & D(F) \subset L^2(\Omega) & \to & \mathcal{L}(H^{3/2}(\partial\Omega_D); H^{1/2}(\Gamma_1)) \\ & C & \mapsto & \Lambda_C \end{array}$$

where Λ_C is the map that takes U into $(J_n\cdot\nu)|_{\Gamma_1}$, by solving the decoupled system (11). Notice that Λ_C derives from $\Sigma_C'(0)$ if we take into account the simplifying assumptions *A1)* and *A2)*.

Since $V = V_{\rm bi}(x)$ is known at $\partial\Omega_D$, the current data $J_n\cdot\nu = \mu_n e^{V^0}u_\nu$ at Γ_1 (output) can be directly replaced by the Neumann data u_ν. Therefore, the inverse problem can be divided into two distinct steps:

Identification Problem 2.2 (Unipolar Case).

1) Define $\gamma := e^{V^0}$ and identify γ from the DtN map $\Lambda_\gamma : U \mapsto \gamma u_\nu|_{\Gamma_1}$, where u solves

$$\operatorname{div}(\gamma \nabla u) = 0 \ \text{ in } \Omega\,, \qquad u = U \ \text{ on } \partial\Omega_D\,, \qquad u_\nu = 0 \ \text{ on } \partial\Omega_N;$$

2) Obtain the doping profile C from: $C(x) = \gamma(x) - \lambda^2 \Delta\,(\ln \gamma(x))$, $x \in \Omega$.

The evaluation of C from γ can be explicitely performed (a direct problem) and is a well posed procedure. The identification issue in Problem 2.2 (1) corresponds to the *electrical impedance tomography* in elliptic equations with mixed boundary data. For the case of the full DtN operator, i.e., $\Gamma_1 = \partial\Omega_D = \partial\Omega$, this inverse problem has been intensively analyzed in the literature (see, e.g., [2, 19] for a survey).

The doping profile identification problem in the bipolar case can be formulated in an analogous way:

Identification Problem 2.3 (Bipolar Case).

1) Define $\gamma := e^{V^0}$ and identify γ from the DtN map $\Phi_\gamma : U \mapsto (\mu_n \gamma u_\nu - \mu_p \gamma^{-1} v_\nu)|_{\Gamma_1}$, where (u, v) solve the coupled system

$$\operatorname{div}(\mu_n \gamma \nabla u) = Q_0(u+v) \ \text{ in } \Omega\,, \qquad u = -U \ \text{ on } \partial\Omega_D\,, \qquad u_\nu = 0 \ \text{ on } \partial\Omega_N;$$

$$\operatorname{div}(\mu_p \gamma^{-1} \nabla v) = Q_0(u+v) \ \text{ in } \Omega\,, \qquad v = U \ \text{ on } \partial\Omega_D\,, \qquad v_\nu = 0 \ \text{ on } \partial\Omega_N;$$

2) Obtain the doping profile C from: $C = \gamma - \gamma^{-1} - \lambda^2 \Delta\,(\ln \gamma)$.

3 Inverse doping profile: Identification issue

In this section we consider some theoretical aspects of the inverse doping profile problem. Despite the encouraging numerical results of Sections 4 and 5, at present, we do not have a theoretical result showing uniqueness of the doping profile from V-C data measured on distinct sub-domains of the boundary. We do present, however, a reasoning that support the conjecture of an identifiability result for the doping profile. The first one is based on recent results due to Bukhgeim and Uhlmann [3] on global uniqueness for the local Dirichlet-to-Neumann map. The second one concerns a discretized version of the problem that falls within the scope of identifying the potential of a discretized Schrödinger equation using external measurements. We treat this problem using techniques from the so-called isotropic case of diffuse tomography [16, 17].

3.1 Global uniqueness approach

In this paper we are considering Ω (the semiconductor) to be 2-dimensional, unless stated otherwise. Therefore, each current measurement is given by a function of one space variable defined on $\Gamma_1 \subset \partial\Omega$. Obviously, a single measurement is not sufficient to identify the doping profile $C : \Omega \subset \mathbb{R}^2 \to \mathbb{R}$. However, adapting some results from [24], related to electrical impedance tomography, we argue that the knowledge of the operator F in Subsection 2.2 (full data case) is enough to determine C uniquely.

We argue as follows: Let V^0 be the solution of the Poisson equation at equilibrium in (11). Given an input voltage $U \in H^{3/2}(\partial\Omega_D)$, the output current can be identified (after rescaling) with the Neumann data of u at Γ_1, i.e., $u_\nu|_{\Gamma_1} = \Lambda_C(U)$, where u is the solution of the elliptic equation in (11). From standard results in elliptic theory, one concludes that for a domain Ω with Lipschitz boundary, there is a one to one relation between the solutions $V^0 \in H^2(\Omega)$ of the Poisson equation and the potentials $C \in L^2(\Omega)$. Therefore, it is enough to consider the problem of

identifying the potential V^0 in (11) or, equivalently, the conductivity $\gamma = e^{V^0}$ as stated in Problem 2.2. The problem of identifying conductivities from the DtN map was analyzed by Nachman in [24]. The next Lemma corresponds to an adaptation of his result to Identification Problem 2.2.

Lemma 3.1. *Let $\Omega \subset \mathbb{R}^2$ be bounded with Lipschitz boundary. Further, let $\Gamma_1 = \partial\Omega_D = \partial\Omega$ and let C_1, C_2, be given two doping profiles such that the corresponding conductivities satisfy*

$$\gamma_1, \gamma_2 \in D(F) := \{\gamma \in W^{2,p}(\Omega),\ p > 1;\ \gamma_+ \geq \gamma(x) \geq \gamma_- > 0 \ \textit{a.e. in}\ \Omega\}\,.$$

Then, the equality $\Lambda_{\gamma_1} = \Lambda_{\gamma_2}$ implies $C_1 = C_2$.

The result of Nachman mentioned above was recently improved by Astala and Päivärinta [1], who proved that any L^∞ conductivity in two dimensions can be determined uniquely from the DtN map.

We address yet another identification result (for the inverse doping profile problem) based on the global uniqueness approach. What concerns uniqueness results for the DtN operator with partial boundary data, the next lemma corresponds to the state of the art (see [3]). This time we consider domains $\Omega \subset \mathbb{R}^3$ with regular boundary and, moreover, $\partial\Omega = \partial\Omega_D = \Gamma_0 \cup \Gamma_1$, i.e., the contacts where the voltage is prescribed (Γ_0) and where the current is measured (Γ_1) overlap.

Lemma 3.2. *Let $\Omega \subset \mathbb{R}^n$, with $n \geq 3$, be a bounded domain with C^2 boundary. Further, let $\xi \in \mathbb{R}^n$ with $\|\xi\| = 1$ and $\varepsilon > 0$ be given. We define*

$$\Gamma_0 := \{x \in \partial\Omega;\ \langle \nu(x), \xi\rangle > -\varepsilon\}, \quad \Gamma_1 := \{x \in \partial\Omega;\ \langle \nu(x), \xi\rangle < \varepsilon\}$$

where $\nu(x)$ is the unit normal vector at $x \in \partial\Omega$ (notice that $\Gamma_0 \cap \Gamma_1 \neq \emptyset$). Moreover, let C_1, C_2 be doping profiles such that the corresponding conductivities satisfy $\gamma_1, \gamma_2 \in C^2(\overline{\Omega})$ and $\gamma_j(x) \geq \gamma_- > 0$ a.e. in Ω, $j = 1, 2$.

Then, the equality $\Lambda_{\gamma_1} = \Lambda_{\gamma_2}$ implies $C_1 = C_2$.

3.2 The Discrete Schrödinger Equation with Partial DtN Data

In this section we consider the characterization problem for the Schrödinger operator potential V given partial information on the Dirichlet-to-Neumann map Λ^V associated to the problem

$$\begin{cases} -\Delta w + Vw = 0 \text{ in } \Omega \\ w\big|_{\partial\Omega} = \phi \end{cases} \tag{12}$$

It is well-known that the change of variables

$$w = \gamma^{1/2} u \quad \text{and} \quad V = \gamma^{-1/2}\Delta\gamma^{1/2} \tag{13}$$

establishes a $1-1$ correspondence between the solutions of (12) and those of

$$\begin{cases} \mathrm{d}iv(\gamma\nabla u) = 0 \text{ in } \Omega \\ u\big|_{\partial\Omega} = \gamma^{-1/2}\big|_{\partial\Omega}\phi \end{cases} \tag{14}$$

The Dirichlet-to-Neumann map for (12) is related to that of (14) by

$$\Lambda^V(\phi) = \gamma^{-1/2}\Lambda_\gamma(\gamma^{-1/2}\phi) + \frac{1}{2\gamma}\frac{\partial\gamma}{\partial n}\phi\ . \tag{15}$$

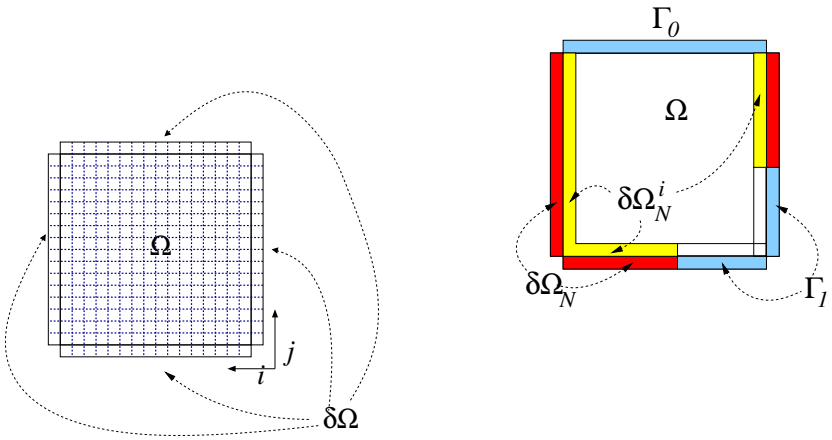

(a) The discretized region $\mathbf{\Omega}$ under consideration and its boundary $\partial\mathbf{\Omega}$.

(b) The boundary conditions imposed in the semi-conductor modeling.

Figure 2: The discretization and the boundary conditions.

It is clear that the knowledge of the DtN map Λ^V for Equation (12) is equivalent to knowledge of its counterpart Λ_γ for (14). Furthermore, any restriction of Λ^V to ϕ supported on a subset Γ_0 of the boundary corresponds to the restriction of Λ_γ supported on this set Γ_0. If we consider current measurements taken in a subset Γ_1 contained in $\partial\Omega$, then, at the level of Λ^V this means that we will only consider the information from Λ^V on Γ_1. Let us call such map $\Lambda^V\big|_{\Gamma_0,\Gamma_1}$.

To the best of our knowledge, there is no characterization result of V based on $\Lambda^V\big|_{(\Gamma_0,\Gamma_1)}$ when $\Gamma_0 \cap \Gamma_1 = \emptyset$. We explore here the discrete analogue of the Dirichlet-to-Neumann characterization problem with partial data for the Schrödinger operator. In this context we consider a discretization $V_{ij} = V(x_i, y_j)$ of $V : \Omega \to \mathbb{R}$ for $(i,j) \in \mathbf{\Omega} \stackrel{\text{def}}{=} \{(i,j) | 1 \le i,j \le N, i,j \in \mathbb{Z}\}$. For a mesh size $\Delta x = \Delta y = \epsilon$, the first equation in (12) is replaced by

$$u_{ij} = \frac{1}{4+\epsilon^2 V_{ij}}(u_{i+1,j} + u_{i-1,j} + u_{i,j+1} + u_{i,j-1}) \qquad \text{for } (i,j) \in \mathbf{\Omega}\ , \tag{16}$$

We define $w_{ij} = 4/(4+\epsilon^2 V_{ij})$ and consider the set of equations described by

$$u_{ij} - \frac{w_{ij}}{4}\left(u_{i+1,j} + u_{i-1,j} + u_{i,j+1} + u_{i,j-1}\right) = 0 \ \text{,where } (i,j) \in \mathbf{\Omega}. \tag{17}$$

We remark that except for minor modifications, in what follows, we could use $1 \le i \le N_1$ and $1 \le j \le N_2$. See Figure 2

The system of equations defined by (17) must be supplemented with suitable boundary conditions. In [16, 17], Dirichlet type boundary conditions were imposed for $u_{i,j}$ whenever $(i,j) \in \partial\mathbf{\Omega}$, where $\partial\mathbf{\Omega}$ is the set of points (i,j) with $0 \le i,j \le N+1$ where either $i \in \{0, N+1\}$ or $j \in \{0, N+1\}$, but not both. See Figure 2. More precisely, in [16, 17] one imposes the condition

$$u_d = \delta_d \quad \forall d = (i_0, j_0) \in \partial\mathbf{\Omega}\ , \tag{18}$$

where $\delta_d(l) \stackrel{\text{def}}{=} 1$ if $d = l$ and 0 otherwise.

If $0 \leq w_{ij} \leq 1$ for all $(i,j) \in \mathbf{\Omega}$, then the problem (17) with boundary conditions (18) has a natural probabilistic interpretation. Namely, u_{ij} represents the probability that a particle undergoing a random walk with absorption will reach the site $d = (i_0, j_0)$ given that at each site $\alpha = (\alpha_1, \alpha_2)$ it has a survival probability w_α for $\alpha \in \mathbf{\Omega}$. See [16]. We remark that a sufficient condition for $w_{ij} \in (0,1)$ is that $V_{ij} > 0$. In what follows we will rely heavily on such interpretation and the notation presented in [16, 17]. In fact, we shall extend some of the results therein so as to allow for the more general boundary conditions that appear in the identification of the doping profile. We refer the reader to Figure 2 where the different boundary conditions are depicted.

The boundary region $\partial\mathbf{\Omega}$ will be decomposed into two parts, $\partial\mathbf{\Omega}_N$ and $\partial\mathbf{\Omega}_D$. On $\partial\mathbf{\Omega}_N$ homogeneous Neumann boundary conditions will be imposed. In this discretized setting, this means that the values of u_α on pixels $\alpha \in \partial\mathbf{\Omega}_D$ and on the adjacent one $\alpha' \in \partial\mathbf{\Omega}_D^i$ coincide. The region $\partial\mathbf{\Omega}_D$ will be further subdivided into two regions Γ_0 and Γ_1. On Γ_0 we will impose nonhomogeneous Dirichlet data whereas on Γ_1 we impose homogeneous Dirichlet data. The measurements correspond to normal derivatives on Γ_1. In other words, $u_\alpha - u_{\alpha'}$ for $\alpha \in \Gamma_1$ and $\alpha' \in \Gamma_1^i$ with α' adjacent to α. Since $u_\alpha = 0$ for $\alpha \in \Gamma_1$ this corresponds to evaluating $u_{\alpha'}$ for $\alpha' \in \Gamma_1^i$.

The first natural question to be addressed is the well posedness of the direct problem. It is answered by the following:

Proposition 3.3. *Given a distribution of values $w = (w_{i,j})_{1 \leq i,j \leq N} \in (0,1)^{N \times N}$ the system of equations in (17) endowed with the boundary conditions*

$$u_\alpha = u_{\alpha'} \text{ for } \alpha \in \partial\mathbf{\Omega}_N \text{ adjacent to } \alpha' \in \partial\mathbf{\Omega}_N^i \tag{19}$$

$$u_\beta = \delta_d \text{ for } \beta \in \Gamma_0 \tag{20}$$

$$u_\gamma = 0 \text{ elsewhere on } \partial\mathbf{\Omega}\ , \tag{21}$$

has a unique solution for each $d \in \Gamma_0$. Furthermore, this solution depends rationally on the components of the array w.

Proof: Let us notice that we have a (sparse) system of N^2 equations in the N^2 unknowns $((u_{ij}))$. The equations for the sites (i,j) with $2 \leq i,j \leq N-1$ are precisely those given by (17), whereas for the sites $\alpha' = (i,j) \in \partial\mathbf{\Omega}_N^i$ or $\partial\mathbf{\Omega}_D^i$ require us to use the boundary conditions. The variables u_α in the site α adjacent to $\alpha' \in \partial\mathbf{\Omega}_N^i$ coincides with $u_{\alpha'}$. Thus, the corresponding equation has to be modified accordingly. On the other hand, if $\alpha' \in \partial\mathbf{\Omega}_D^i$ then the value of u_α must be $\delta_d(\alpha)$. In the sites adjacent to the Dirichlet boundary, or in the interior sites, the diagonal element of the matrix representing the system (17) is 1. On the sites adjacents to the Neumann boundary the value of w_{ij} must be changed to $w_{ij}/(1-(w_{ij}/4))$. In either case, after incorporating the boundary conditions (of mixed Neumann and Dirichlet type) the matrix representing the problem is strictly diagonally dominant. Thus the system of equations is solvable and possesses a unique solution, which depends rationally on the coefficients w_{ij}. *Q. E. D.*

Remark 3.4. *The assumption $w_{ij} \leq 1$ for all i and j is crucial for the above argument. This is ensured, for example, if $V_{ij} > 0$ for all i and j, which in turn can be guaranteed if $V(x)$ is positive.*

Remark 3.5. *The vanishing Neumann boundary conditions can be recast so as to preserve the probabilistic interpretation of the problem as follows: Suppose that $(i,j) \in \partial\mathbf{\Omega}_N^i$ is adjacent to $(i-1,j) \in \partial\mathbf{\Omega}_N$ (similar considerations hold at the*

other points $(i,j) \in \partial\mathbf{\Omega}^i_N$*). Then, the Equation (17) for this site becomes*

$$u_{ij} = \frac{w_{ij}}{4 - w_{ij}} \left(u_{i+1,j} + u_{i-1,j} + u_{i,j+1} + u_{i,j-1}\right) = 0 \ . \tag{22}$$

Remark 3.6. *Since the variable* $u_{i-1,j}$ *and the coefficient* $w_{i,j}$ *do not appear in any other equation in the system, we could reinterpret Equation (22) as*

$$u_{ij} = \frac{w^{\text{eff}}_{ij}}{3} \left(u_{i+1,j} + u_{i-1,j} + u_{i,j+1} + u_{i,j-1}\right) = 0 \ .$$

with $w^{\text{eff}}_{ij} = 3w_{ij}/(4 - w_{ij})$*. Notice that* $w^{\text{eff}}_{ij} \in (0,1)$ *if* $w_{ij} \in (0,1)$*. Thus, for all practical purposes, the equations associated to the Neumann boundary sites could be replaced by equivalent equations with vanishing Dirichlet boundary conditions.*

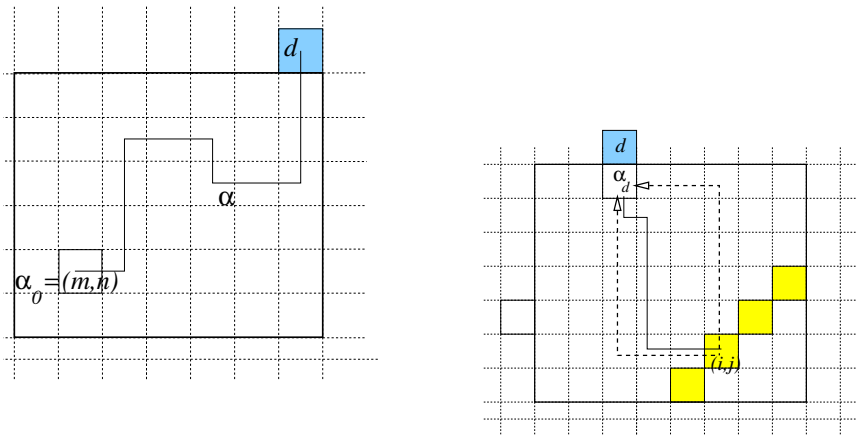

(a) An example of a path α connecting an internal point to a boundary point d.

(b) An example of a few minimal length paths connecting an internal point to the point α_d adjacent to a detector d.

Figure 3: The paths.

Remark 3.7. *In [16] a crucial role is played by the probabilistic interpretation of the system of equations (17) in the solution of the inverse problem of the so-called isotropic diffuse tomography problem. See also [27]. In particular, the following Feynman-Kac type formula holds for a fixed* $d \in \Gamma_0$

$$u_{mn} = \sum_{\alpha \in \mathcal{P}^d_{(m,n)}} \prod_{s \in \alpha} t^{\alpha_{s+1}}_{\alpha_s} \ ,$$

where $\mathcal{P}^d_{(m,n)}$ *denotes the set of all paths connecting the site* (m,n) *to the boundary site* d*, and a path* α *consists of an ordered set of successively adjacent sites starting at a neighbor to* (m,n) *and ending at* d*, and* $t^{\alpha_{s+1}}_{\alpha_s}$ *denotes the transition probability from the site* α_s *to the site* α_{s+1}*. Thus,* $t^{\alpha_1}_{\alpha_0} = w_{mn}/4, \cdots$*.*

We now turn our attention to the inverse problem. We define the restricted (discrete) DtN map $\Lambda^w_{\Gamma_0,\Gamma_1}$ which sends Dirichlet data supported on Γ_0 to Neumann

measurements on Γ_1. Our next goal is to prove an identification result that is similar in spirit to the main result of [16]. It implies that in the discrete context, and under suitable hypothesis on the potential, one can determine such potential in the interior of a region defined by the current measurement boundary using voltage to current measurements. The larger the boundary Γ_1 in Figure 2.b, the larger the region where the potential can be uniquely determined from voltage to current measurements provided the total length of Γ_1 is smaller than the size of the side. More precisely, we have the following:

Theorem 3.8. *For a dense open set of values $w \in (0,1)^{N\times N}$, the map $\Lambda^w_{\Gamma_0,\Gamma_1}$ uniquely determines the values of w_{ij} for $(i,j) \in \mathbf{\Omega}$ satisfying $2 \le i+j \le p'+1$, $2p' \le N+1$, provided the support of the Dirichlet data contains the points $(N+1,N),\cdots,(N+1,N-p'+1)$ and p' is smaller than the size of one of the sides of Γ_1.*

Proof: The argument follows closely that of [16] by proceeding along the diagonals. The p-th diagonal is defined by the sites$(i,j) \in \mathbf{\Omega}$ such that

$$i+j = p+1\ .$$

For instance, the very first diagonal, associated to $p=1$, leads to the equation

$$\widehat{V}_{11} z^d_{11} - (z^d_{12} + z^d_{10} + z^d_{01} + z^d_{21}) = 0 \tag{23}$$

where (z^d_{ij}) denotes the solution of system (17) with boundary conditions (19)–(21), and Dirichlet data specified as δ_d for $d \in \Gamma_0$. Furthermore, we shall use the notation $\widehat{V}_{ij} \stackrel{\text{def}}{=} 4/w_{ij}$. In this simple case, we see that in Equation (23) $z^d_{10} = z^d_{01} = 0$ and $z^d_{11}, z^d_{12}, z^d_{21}$ are all boundary measurements, and thus we can recover $\widehat{V}_{11}$. The next diagonal ($p=2$) yields for each detector d:

$$\begin{aligned} \widehat{V}_{12} z^d_{12} - (z^d_{13} + z^d_{11} + z^d_{02} + z^d_{22}) &= 0 \\ \widehat{V}_{21} z^d_{21} - (z^d_{22} + z^d_{20} + z^d_{11} + z^d_{21}) &= 0 \end{aligned}$$

Here the unknowns are $\widehat{V}_{12}$, $\widehat{V}_{21}$, and z^d_{22}. The remaining variables, z^d_{12}, z^d_{21}, z^d_{13}, z^d_{11}, z^d_{20}, z^d_{02} are all boundary values or known from the measurements. Upon choosing two distinct detectors we are led to the system:

$$\left\{ \begin{array}{rcl} \widehat{V}_{12} z^{d_1}_{12} - (z^{d_1}_{13} + z^{d_1}_{11} + z^{d_1}_{02} + z^{d_1}_{22}) &=& 0 \\ \widehat{V}_{21} z^{d_1}_{21} - (z^{d_1}_{22} + z^{d_1}_{20} + z^{d_1}_{11} + z^{d_1}_{21}) &=& 0 \\ \widehat{V}_{12} z^{d_2}_{12} - (z^{d_2}_{13} + z^{d_2}_{11} + z^{d_2}_{02} + z^{d_2}_{22}) &=& 0 \\ \widehat{V}_{21} z^{d_2}_{21} - (z^{d_2}_{22} + z^{d_2}_{20} + z^{d_2}_{11} + z^{d_2}_{21}) &=& 0\ , \end{array} \right. \tag{24}$$

where the unknown is $(\widehat{V}_{12}, \widehat{V}_{21}, z^{d_1}_{22}, z^{d_2}_{22})$. The system has a unique solution iff its determinant, which is given by $z^{d_1}_{12} z^{d_2}_{21} - z^{d_1}_{21} z^{d_2}_{12}$ does not vanish. In this case, as a byproduct of the solution we also determine $z^{d_1}_{22}$ and $z^{d_2}_{22}$. The latter will be used in the next step, together with a possible collection of other values of z^d_{22} for $d \in \{d_1, d_2, \cdots, d_{\max}\}$. In general, for $p \ge 1$, the equations associated to $i+j = p+1$ and detector d take the form

$$\left\{ \begin{array}{rcl} \widehat{V}_{1,p} z^d_{1,p} - (z^d_{1,p+1} + z^d_{1,p-1} + z^d_{0,p} + z^d_{2,p}) &=& 0 \\ \widehat{V}_{2,p-1} z^d_{2,p-1} - (z^d_{2,p} + z^d_{2,p-2} + z^d_{1,p-1} + z^d_{3,p-1}) &=& 0 \\ \vdots &=& \vdots \\ \widehat{V}_{p-1,2} z^d_{p-1,2} - (z^d_{p-1,3} + z^d_{p-1,1} + z^d_{p-2,2} + z^d_{p,2}) &=& 0 \\ \widehat{V}_{p,1} z^d_{p,1} - (z^d_{p,2} + z^d_{p,0} + z^d_{p-1,1} + z^d_{p+1,1}) &=& 0 \end{array} \right. \tag{25}$$

Notice that if we assume that the values of $z^d_{i',j'}$ have all been determined (or measured) for $i'+j' \leq p+1$ then the unknowns become

$$\widehat{V}_{1,p}, \widehat{V}_{2,p-1}, \cdots, \widehat{V}_{p,1} \text{ and } z^d_{1,p+1}, z^d_{2,p}, \cdots, z^d_{p+1,1} \ .$$

We now order the detectors $d_1, d_2, \cdots, d_m$, successively from left to right, on the region Γ_0 of Figure 2(b). By detectors we mean positions where the Dirichlet data is taken to be $\delta_d(i,j)$. [2] The given data consists of the currents in the region adjacent to Γ_1. Since on Γ_1 we have $u=0$, knowledge of the currents tantamounts to knowledge of the values of u^d_α for $\alpha \in \{0\} \times \{1, \cdots, p'\}$ or $\alpha \in \{1, \cdots, p'\} \times \{0\}$.

We now introduce the following inductive hypothesis:
H1: For a generic (open and dense) set $\mathcal{A}$ of the space of unknowns $((\widehat{V}_{ij})) \in (1,\infty)^{N\times N}$ one can solve the system of equations (25) for the variables z^d_{ij} with $i+j \leq p+2$, $d \in \{d_1, d_2, \cdots, d_p\}$, and $\widehat{V}_{ij}$ for $i+j \leq p+1$ in terms of the given data.

In the present context, by data we mean the values of z^d_{ij} for which any of the indices i or j belongs to the set $\{0,1\}$ and $d \in \{d_1, d_2, \cdots, d_p\}$. The validity of the induction hypothesis for $p=1$ derives from the remark following Equation (23) above. The inductive step relies on the fact that in order to go from p to $p+1$ we have to solve a system of equations based on (25) for detectors $d_1, \cdots, d_p$. This in turn, is equivalent to showing that the determinant

$$D_p \stackrel{\text{def}}{=} \begin{vmatrix} z^{d_1}_{1,p} & z^{d_2}_{1,p} & z^{d_3}_{1,p} & \cdots & z^{d_{p-1}}_{1,p} & z^{d_p}_{1,p} \\ z^{d_1}_{2,p-1} & z^{d_2}_{2,p-1} & z^{d_3}_{2,p-1} & \cdots & z^{d_{p-1}}_{2,p-1} & z^{d_p} \\ \vdots & \vdots & \vdots & \vdots & \vdots & \vdots \\ z^{d_1}_{p-1,2} & z^{d_2}_{p-1,2} & z^{d_3}_{p-1,2} & \cdots & z^{d_{p-1}}_{p-1,2} & z^{d_p}_{p-1,2} \\ z^{d_1}_{p,1} & z^{d_2}_{p,1} & z^{d_3}_{p,1} & \cdots & z^{d_{p-1}}_{p,1} & z^{d_p}_{p,1} \end{vmatrix} \tag{26}$$

does not vanish in the set $\mathcal{A}$. Although the technique we employ here is the very same used in [16], the crucial difference is that in our case the determinant D_p consists of detectors on the opposite side from where the measurements are being taken. More precisely, we show that the analytic function $D_p(w)$ is not identically zero in a neighborhood of $w=0$. Another difference from the situation in [16] is the fact that we have Neumann type boundary conditions in part of the boundary. This, however, causes no further difficulty at the light of Remark 3.5.

To complete the proof, it thus remain to show that if we take all values of $w_{ij} = \rho$ and let $\rho \to 0$, then under the assumption that $p \leq p'$, $D_p = A(p)\rho^{L(p)} + \mathcal{O}(\rho^{L(p)}+1)$ with $A(p) \neq 0$ and $L(p)$ depending only on geometric parameters associated to the size of the grid and the location of the detectors and the diagonal p. To prove this claim, we start by noticing that because of Remark 3.7, when $\rho \to 0$, we have $z^d_{ij}(\rho) = A^{d,p}_{i,j}\rho^{\ell(p,i,j)+1} + \mathcal{O}(\rho^{\ell(p,i,j)+2})$, where $\ell(p,i,j)$ is the length of the smallest path connecting the site (i,j) to the point α_d in Γ_0 adjacent to the detector d. See Figure 3(b). Furthermore, $A^{d,p}_{i,j}$ denotes the number of paths in the region $\mathbf{\Omega}$ of minimal length $\ell(p,i,j)$ connecting (i,j) to α_d. If we assume that the coordinates of $\alpha_d = (i',j')$ then it is easy to check that $\ell(p,i,j) = |i'-i| + |j'-j|$ and that the number of such paths is given by

$$A^{d,p}_{i,j} = \begin{pmatrix} |i'-i|+|j'-j| \\ |i'-i| \end{pmatrix} = \begin{pmatrix} \ell(p,i,j) \\ |i'-i| \end{pmatrix} = \begin{pmatrix} \ell(p,i,j) \\ |j'-j| \end{pmatrix} \tag{27}$$

A straightforward combinatorial argument gives that $A(p) \neq 0$ provided $2p' \leq N+1$. [3]

[2] We recall that in the region Γ_0 we control the voltages and by placing such detectors in this region we are defining a basis for the space of input voltages.

[3] The hypothesis that $2p' \leq N+1$ is crucial, and although it seems it could be relaxed we

4 The Landweber-Kaczmarz method

In this section we discuss a numerical approach for doping profile identification in the linearized unipolar case close to equilibrium (see Problem 2.2). As discussed in Subsection 2.2, the main task in this inverse problem is the identification of the coefficient γ in the elliptic PDE

$$\operatorname{div}(\gamma \nabla u) = 0 \ \text{ in } \Omega\,, \qquad u = U \ \text{ on } \partial\Omega_D\,, \qquad u_\nu = 0 \ \text{ on } \partial\Omega_N\,. \tag{28}$$

The second step in Identification Problem 2.2 can be carried out in a straightforward way. Thus, we can reduce the inverse doping profile problem in the linearized unipolar case to the problem of identifying $\gamma(x)$ in (28) from the Dirichlet to Neumann (DtN) map

$$\begin{array}{rccc} \Lambda_\gamma: & H^{3/2}(\partial\Omega_D) & \to & H^{1/2}(\Gamma_1) \\ & U & \mapsto & \gamma\, u_\nu|_{\Gamma_1} \end{array} \tag{29}$$

Notice that, due to the nature of the boundary conditions related to the practical experiments, we have to restrict the domain of definition of the DtN operator to the linear subspace $D(\Lambda_\gamma) := \{U \in H^{3/2}(\partial\Omega_D);\, U|_{\Gamma_1} = 0\}$. Furthermore, the measurements (Neumann data) are only available at Γ_1.

This is the essential difference between the parameter identification problem in (28) and the inverse problem in *electrical impedance tomography*, namely the fact that both Dirichlet and Neumann data are known only at specific parts of the boundary. For this particular type of DtN operators there are so far no analytical results concerning identifiability and, to our knowledge, the few numerical results in the literature are those discussed in [4, 5, 6, 13].

In this section we shall work within the following framework:

- Parameter space: $\mathcal{X} := L^2(\Omega)$;
- Input (fixed): $U_j \in H^{3/2}(\partial\Omega_D)$, with $U_j|_{\Gamma_1} = 0$, $1 \le j \le N$;
- Output (data): $Y = \{\Lambda_\gamma(U_j)\}_{j=1}^N \in \left[L^2(\Gamma_1)\right]^N =: \mathcal{Y}$;
- Parameter to output map: $\begin{array}{rccc} F: & D(F) \subset \mathcal{X} & \to & \mathcal{Y} \\ & \gamma(x) & \mapsto & \{\Lambda_\gamma(U_j)\}_{j=1}^N \end{array}$

where the domain of definition of the operator F is

$$D(F) := \{\gamma \in L^2(\Omega);\, \gamma_+ \ge \gamma(x) \ge \gamma_- > 0, \text{ a.e. in } \Omega\}$$

(here γ_- and γ_+ are appropriate constants). We shall denote noisy data by Y^δ and assume that the data error is bounded by $\|Y - Y^\delta\| \le \delta$. Thus, we are able to represent the inverse doping problem in the general form

$$F(\gamma) = Y^\delta. \tag{30}$$

The next lemma describes some crucial properties of the operator F, that will be necessary for the analysis of the iterative methods discussed in this paper. Here, only a sketch of the proof of Lemma 4.1 is given, for details see [5].

Lemma 4.1. *Let the voltages $\{U_j\}_{j=1}^N$ be chosen in the neighborhood of $U \equiv 0$. The parameter-to-output map F defined above is well-defined and Fréchet differentiable on $D(F)$.*

Proof: The first statement follows from the well-definedness of the V-C map, cf. Lemma 2.1. The Fréchet differentiability of F follows from the differentiability of the V-C map (see Lemma 2.1) together with the differentiability of the map that takes the doping profile C onto the solution (V, u, v) of (8). □

do not have a proof of this fact at the present. We thank C. G. Tamm (IMPA) for enlightening discussions on this combinatorial exercise.

A simple and robust iterative method to solve the inverse problem (30) is the *Landweber iteration* [7, 8, 10, 18], in which the k-th step is described by

$$\gamma_{k+1}^{\delta} \;=\; \gamma_k^{\delta} - F'(\gamma_k^{\delta})^*\big(F(\gamma_k^{\delta}) - Y^{\delta}\big)\,.$$

This iteration is known to generate a regularization method for the inverse problem, the stopping index playing the rôle of the regularization parameter (for regularization theory see, e.g., [8, 9, 10, 29]).

We propose a variation of the Landweber iteration as an alternative to solve the identification problem (28), namely the *Landweber-Kaczmarz method*. This method results from the coupling of the strategies of both the Landweber and the Kaczmarz iterative methods. The motivation for this choice of strategy lays in the fact that the data in (30) consists of a vector of measurements $\{\Lambda_\gamma(U_j)\}_{j=1}^N$ and the principal characteristic of the Kaczmarz method is the minimization, at each iteration step, of a least square functional which takes into account only one component of this measurement vector.

A detailed analysis of the Landweber-Kaczmarz method can be found in [20]. It is worth mentioning that this method has already been successfully applied to *electrical impedance tomography* by Nachman in [24].

To formulate the method, we first need to define the components of the parameter to output map: $F = \{\mathcal{F}_j\}_{j=1}^N$, where

$$\mathcal{F}_j : L^2(\Omega) \supset D(F) \ni \gamma \mapsto \Lambda_\gamma(U_j) \in L^2(\Gamma_1)\,.$$

Now, setting $Y_j^{\delta} := \mathcal{F}_j(\gamma^{\delta})$, $1 \le j \le N$, the Landweber-Kaczmarz iteration can be written in the form

$$\gamma_{k+1}^{\delta} \;=\; \gamma_k^{\delta} - \mathcal{F}_k'(\gamma_k^{\delta})^*\big(\mathcal{F}_k(\gamma_k^{\delta}) - Y_k^{\delta}\big)\,, \tag{31}$$

for $k = 1, 2, \ldots$, where we adopted the notation

$$\mathcal{F}_k := \mathcal{F}_j, \quad Y_k^{\delta} := Y_j^{\delta}, \quad \text{whenever} \quad k = i\,N + j, \quad \text{and} \quad \left\{ \begin{array}{l} i = 0, 1, \ldots \\ j = 1, \ldots, N \end{array} \right. .$$

Notice that each step of the Landweber-Kaczmarz method consists of one Landweber iterative step with respect to the j-th component of the residual in (30). These Landweber steps are performed in a cyclic way, using the components of the residual $\mathcal{F}_j(\gamma) - Y_j^{\delta}$, $1 \le j \le N$, one at a time.

As far as the implementation is concerned, it is enough to describe the general step of the Landweber iteration. The variational formulation of the iterative step in (31) reads

$$\langle \gamma_{k+1} - \gamma_k,\; h\rangle_{L^2(\Omega)} \;=\; -\langle \mathcal{F}_k'(\gamma_k)h,\; \mathcal{F}_k(\gamma_k) - Y_k\rangle_{L^2(\Omega)}\,, \tag{32}$$

where $h \in H^1(\Omega)$ is a test function (to simplify the notation we set $\delta = 0$, i.e., $Y_k^{\delta} = Y_k$ and $\gamma_k^{\delta} = \gamma_k$).

In order to compute the inner product on the right hand side of (32), we use the identity:

$$\langle \mathcal{F}'(\gamma)h, z\rangle_{L^2(\Gamma_1)} \;=\; \int_\Omega h\,\nabla G(\gamma)\cdot\nabla\Phi(\gamma)\,dx, \tag{33}$$

for $z \in L^2(\Gamma_1)$, where the $H^1(\Omega)$-functions $\Phi(a) = w_1$ and $G(a) = w_2$ solve

$$\left\{ \begin{array}{rcll} -\nabla(a(x)\nabla w_1) &=& 0, & \text{in } \Omega \\ w_1 &=& 0, & \text{on } \Gamma_0 \\ w_1 &=& z, & \text{on } \Gamma_1 \\ a(x)\partial w_1/\partial\nu &=& 0, & \text{on } \partial\Omega_N \end{array} \right. \qquad \left\{ \begin{array}{rcll} -\nabla(a(x)\nabla w_2) &=& 0, & \text{in } \Omega \\ w_2 &=& U, & \text{on } \partial\Omega_D \\ a(x)\partial w_2/\partial\nu &=& 0, & \text{on } \partial\Omega_N \end{array} \right.$$

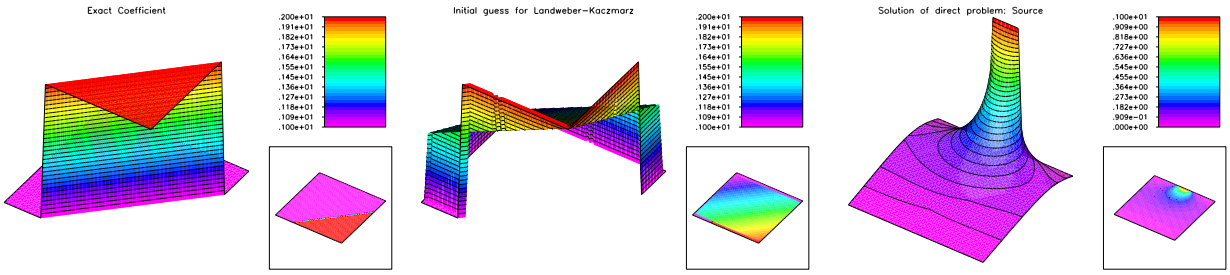

(a) (b) (c)

Figure 4: Picture (a) shows the doping profile to be reconstructed. The initial condition for the Landweber-Kaczmarz method is shown in picture (b). On picture (c) the problem data is shown: A typical source $U(x)$ appears as the Dirichlet boundary condition at $y = 1$ (Γ_0 is the upper right edge). The corresponding current is measured at the contact Γ_1 (lower left edge), where $U(x)$ is assumed to vanish.

respectively. For details on the derivation of (33) see, e.g., [4].

Therefore, the right hand side of (32) can be evaluated by using (33) with $z = \mathcal{F}_k(\gamma_k) - Y_k$. For the concrete numerical test performed in this section, $\Omega \subset \mathbb{R}^2$ is the unit square and the boundary parts are

$$\Gamma_1 := \{(x,1)\,;\ x \in (0,1)\}\,, \quad \Gamma_0 := \Gamma_1 \cup \{(x,0)\,;\ x \in (0,1)\}\,, \quad \partial\Omega_D := \Gamma_0 \cup \Gamma_1\,,$$

$$\partial\Omega_N := \{(0,y)\,;\ y \in (0,1)\} \cup \{(1,y)\,;\ y \in (0,1)\}\,.$$

The fixed inputs U_j vanish at Γ_1 and are chosen to be piecewise constant functions on $\Gamma_0 = \{(x,0)\,;\ x \in (0,1)\}$.

$$U_j(x) := \begin{cases} 1, & |x - x_j| \le h \\ 0, & \text{else} \end{cases}$$

where the points $(x_j, 1)$, $j = 1, \ldots, N$, are uniformly distributed in the segment Γ_0.

To generate the problem data, one has to solve the direct problem in (28) for each input function U_j, $j = 1, \cdots, N$. In order to avoid so-called *inverse crimes* (see [8]), these forward problems are solved using an adaptive refined grid (with approximately 8000 nodal points) while the mixed elliptic boundary value problems, related to the Landweber-Kaczmarz iteration are solved on uniformly refined grids (with approximately 2000 nodal points).

We still have to consider an important issue concerning the stability of the numerical implementation. Due to the choice of Ω, $\partial\Omega_D$ and $\partial\Omega_N$ meet at angles of and $\pi/2$. Thus, the solutions of the mixed boundary value problems in the Landweber-Kaczmarz iteration are not in $H^2(\Omega)$ (see [15] for details). Due to this lack of regularity, the implementation turns out to be very unstable. An alternative to bypass this instability is to make the additional assumption that the doping profile is known in a thin strip close to $\partial\Omega_D$. Therefore, we only have to reconstruct the values of $\gamma(x)$ at a subdomain $\tilde{\Omega} \subset\subset \Omega$. With this extra assumption, the numerical implementation becomes stable and we are able to (numerically) verify local convergence of the Landweber-Kaczmarz iteration. It is worth mentioning that this sort of assumption has been used since the early investigations of the electrical impedance tomography, in order to ensure extra regularity for both numerical and analytical approaches (see [25]).

The setup of the problem is shown in figure Figure 4 The doping profile to be identified is shown in picture (a) – the p-n junction is a straight line. The initial condition for the Landweber-Kaczmarz method is shown in picture (b), while the

solution u of the direct problem for a typical source U is shown in picture (c). In this figure, as well as in the forthcoming ones, Γ_1 appears in the lower right part of the picture and $\partial\Omega_D/\Gamma_1$ appears on the top (the origin corresponds to the upper right corner).

In Figure 5 we show the identification results obtained via the Landweber-Kaczmarz method using noiseless data and different number of (voltage, current) pairs, i.e., different values of N: picture (a) one pair; (b) three pairs; (c) nine pairs; (d) twenty one pairs.

5 A level set type method

In this section we use a level set type method in order to approximate the solution of Identification Problem 2.2. Two experiments are performed: the first one, for comparison purposes, corresponds to the identification problem presented in Section 4 (linear p-n junction with piecewise constant γ); in the second experiment we try to reconstruct a p-n junction parameterized by an analytic function (see Figure 6).

In what follows, the function spaces $\mathcal{X}$, $\mathcal{Y}$ as well as the operators F, Λ_γ and also the sets Ω, $\partial\Omega_D$, $\partial\Omega_N$, Γ_1 are the same as in Section 4. We assume, however, that only one measurement is given, i.e., only one pair of (voltage, current) data is available for the reconstruction. This assumption corresponds to the choice $N = 1$ in the definition of the space $\mathcal{Y}$. The corresponding source function U_1 is shown at Figure 4 (c).

In our numerical experiments we use the level set method introduced in [21, 14]. According to this approach, one represents the p-n junction by the zero level set of a H^1-function $\phi : \Omega \to \mathbb{R}$, in such a way that $\phi(x) > 0$ if $\gamma(x) = 2$ and $\phi(x) < 0$ if $\gamma(x) = 1$ (see Figure 6). Starting from some initial guess $\phi_0 \in H^1(\Omega)$, one solves the Hamilton-Jacobi equation

$$\frac{\partial \phi}{\partial t} + V\nabla\phi = 0 \tag{34}$$

where $V = -v\frac{\nabla\phi}{|\nabla\phi|^2}$ and the *velocity* v solves

$$\begin{cases} \alpha(\Delta - I)v = \frac{\delta(\phi(t))}{|\nabla\phi(t)|}\left[F'(\chi(t))^*(F(\chi(t)) - Y^\delta) - \alpha\nabla\cdot\Big(\frac{\nabla P(\phi)}{|\nabla P(\phi)|}\Big)\right], \text{ in } \Omega \\ \dfrac{\partial v}{\partial \nu} = 0 \text{ , on } \partial\Omega \end{cases} \tag{35}$$

Here, $\alpha > 0$ is a regularization parameter and $\chi = \chi(x,t)$ is the projection of the level set function $\phi(x,t)$ defined by:

$$\chi(x,t) = P(\phi(x,t)) := \begin{cases} 2, & \text{if } \phi(x,t) > 0 \\ 1, & \text{if } \phi(x,t) < 0 \end{cases} .$$

In [14, 21] this level set method was used to reconstruct inclusions $D \subset\subset \Omega$. Notice that, in our case, the set D corresponds to the P-region (see Figure 1) and the condition $\overline{D} \subset \Omega$ is not satisfied. This fact, however, does not affect the derivation of the Hamilton-Jacobi equation (34). Moreover, it does not affect the boundary conditions for the elliptic problem (35) either.

The family $\chi(\cdot,t)$ approximate the doping profile $\gamma(\cdot)$ as $t \to \infty$. This follows from the fact that the solution $\phi(\cdot,t)$ of (34) converges to the minimum of the Tikhonov functional

$$\mathcal{G}_\alpha(\phi) := \|F(P(\phi)) - Y^\delta\|^2_{\mathcal{Y}} + 2\alpha|P(\phi)|_{\mathtt{BV}} + \alpha\|\phi - \phi_0\|^2_{H^1(\Omega)} \tag{36}$$

as $t \to \infty$, for each regularization parameter $\alpha > 0$ (see [14, Definition 2.2] for the precise definition of a minimizer of $\mathcal{G}_\alpha(\phi)$).

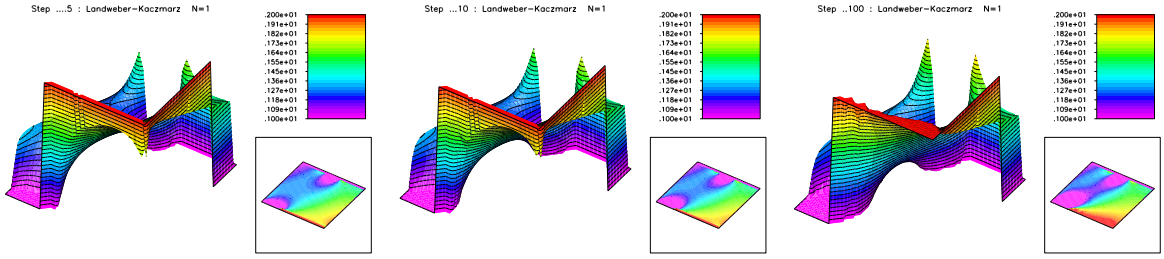

(a)

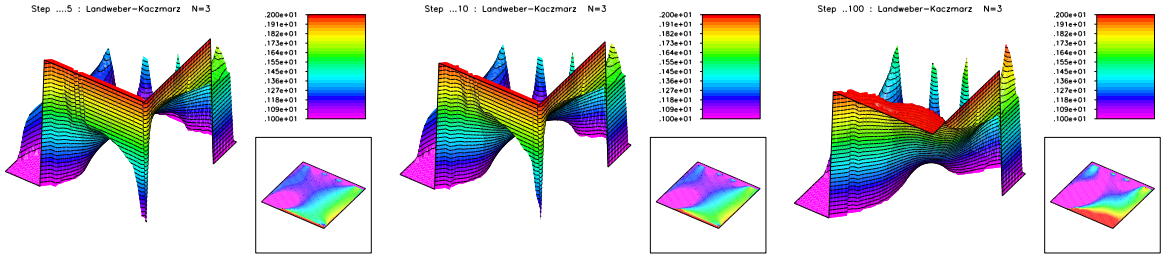

(b)

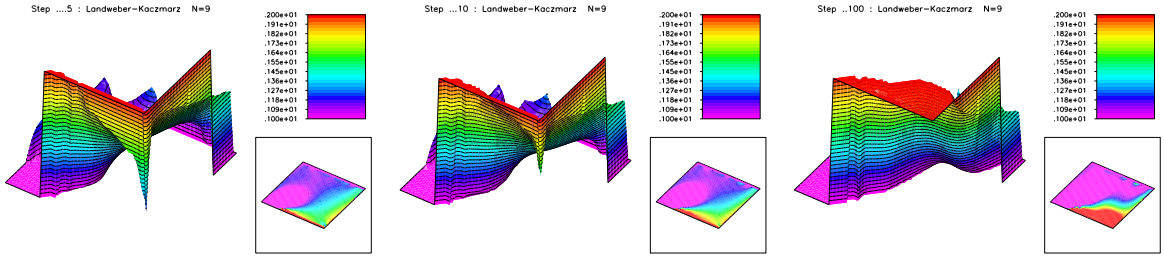

(c)

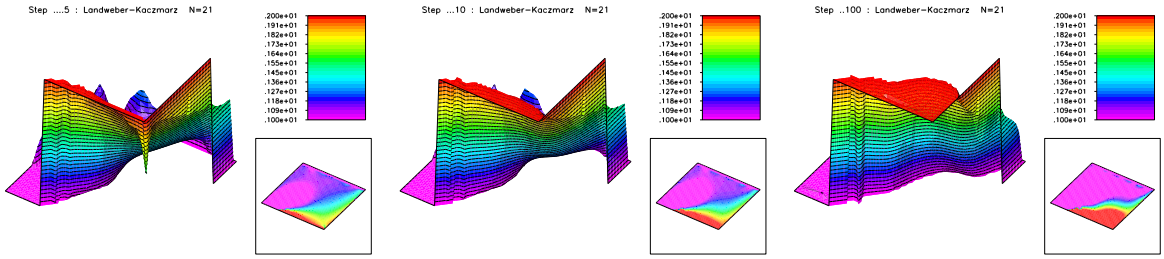

(d)

Figure 5: Different runs of the Landweber-Kaczmarz method. Number of available sources: (a) one, (b) tree, (c) nine, (d) twenty one. The initial condition for all runs is shown in Figure 4 (b).

The next lemma corresponds to specific results selected from [14]. It allows a better understanding of the least-square problem behind the level set formulation and also analytically substantiates the numerical results presented in the sequel.

Lemma 5.1. *Stability, Convergence and Well-Posedness:*

(a) *Let $Y^\delta = Y$ (noiseless case), and let ϕ_α be a minimizer of $\mathcal{G}_\alpha$. Then, for every sequence $\{\alpha_k\}_{k\in\mathbb{N}}$ converging to zero, there exists a subsequence $\{\alpha_{k(l)}\}_{l\in\mathbb{N}}$, such that $\{\phi_{\alpha_{k(l)}}\}_{l\in\mathbb{N}}$ is strongly convergent. Moreover, the limit is a minimal norm solution of (30).*

(b) *Let $\|Y^\delta - Y\|_{\mathcal{Y}} \leq \delta$. If $\alpha = \alpha(\delta)$ satisfies $\lim_{\delta\to 0} \alpha(\delta) = 0$ and $\lim_{\delta\to 0} \frac{\delta^2}{\alpha(\delta)} = 0$, then, for a sequence $\{\delta_k\}_{k\in\mathbb{N}}$ converging to 0, the sequence $\phi_{\alpha(\delta_k)}$ converges to a minimal norm solution of (30).*

(c) *For any given $\phi_0 \in H^1(\Omega)$ the functional $\mathcal{G}_\alpha$ attains a minimizer.*

We conclude this section presenting two different numerical experiments concerning the Identification Problem 2.2. In the first one, the doping profile to be identified is the same as in Section 4, i.e., a linear p-n junction (see Figure 6 (a)). Initially we implement the level set method for the case of exact data. The results are shown in Figure 7 (plots of the error). Notice that the first picture (top left) corresponds to the initial guess. In a second run we added 10% random noise to the exact data and repeated the experiment (see Figure 8). In a second experiment we try to identify a p-n junction parameterized by an analytical function (see Figure 9). Exact data is given.

6 Final comments and conclusions

Differently from the Landweber-Kaczmarz method considered in Section 4, the level set method does not require the assumption that the doping profile is known in some strip close to $\partial\Omega_D$. For this level set approach, only the knowledge of the doping profile at Γ_1 is required in order to obtain a stable performance of the method. This assumption is in no way restrictive, since we need to know γ_ν at Γ_1 in order to implement the DtN map in (29).

We now comment on the amount of information used in the identification. For comparison purposes we implemented the Landweber-Kaczmarz method using different quantity of data, i.e., different number of data voltage-current pairs. In one of the experiments we used a single pair of data. In this case the Landweber-Kaczmarz method reduces to the classical Landweber iteration.

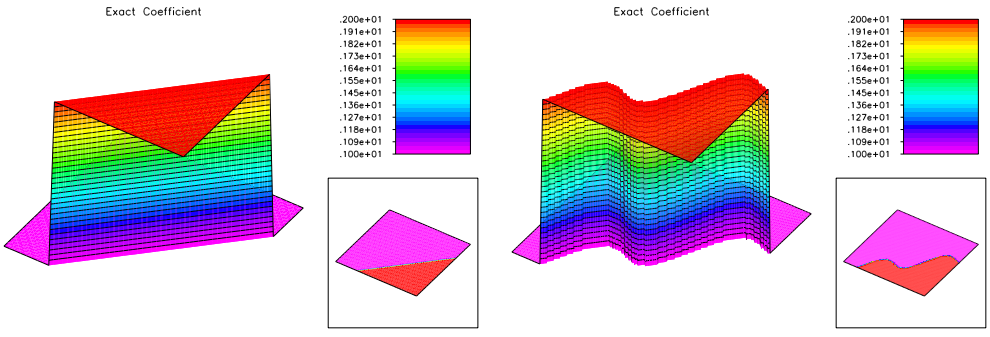

(a) (b)

Figure 6: Pictures (a), (b) show the doping profiles to be reconstructed in the two different experiments for the level set method.

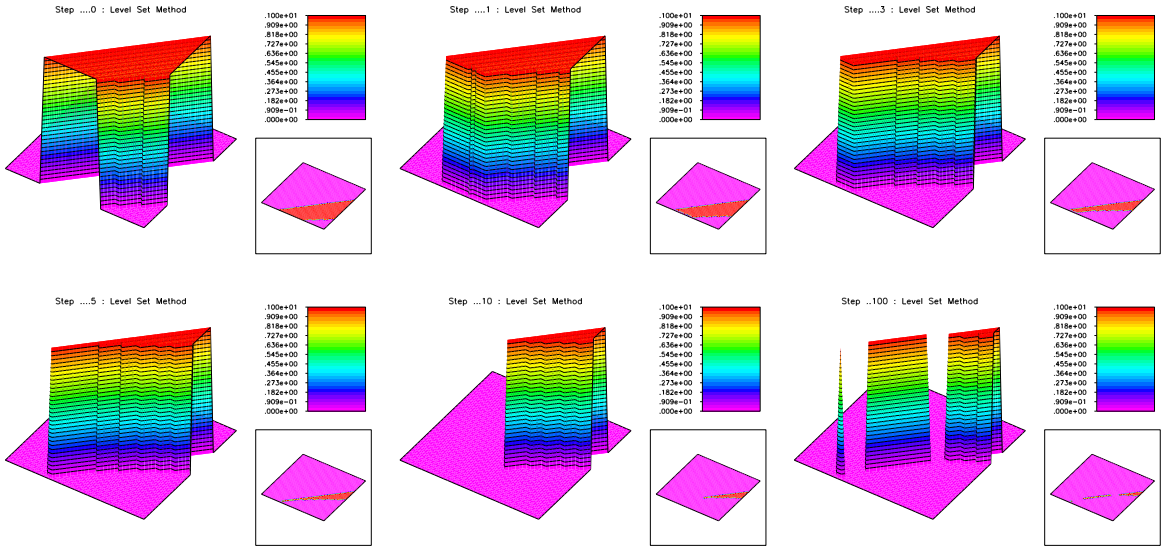

Figure 7: First numerical experiment (linear p-n junction): Evolution of the iteration error for the level set method and exact data.

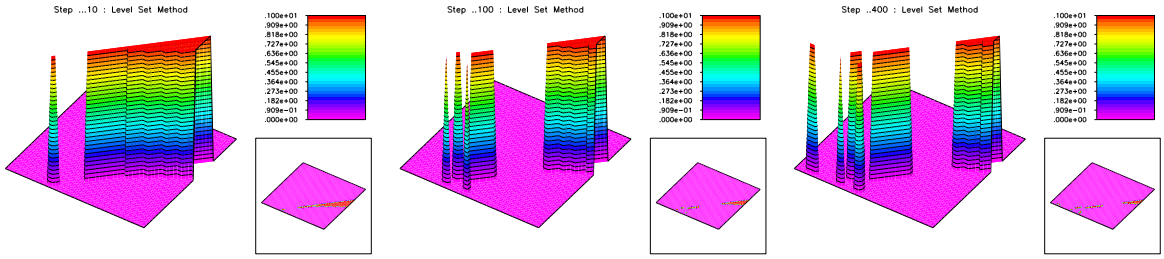

Figure 8: First numerical experiment (linear p-n junction): Evolution of the iteration error for the level set method and data with 10% random noise.

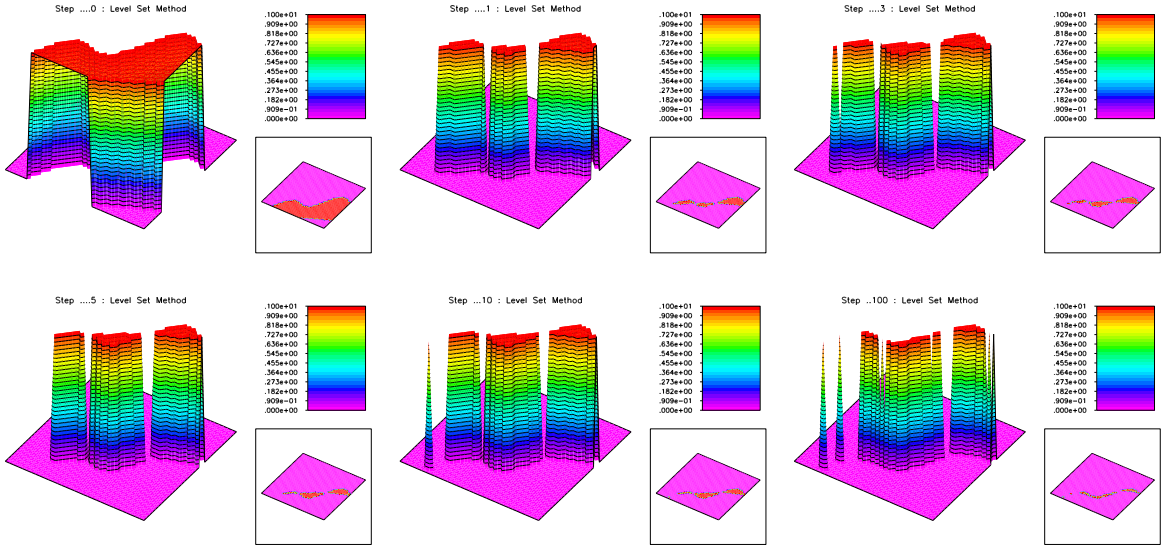

Figure 9: Second numerical experiment (analytical p-n junction): Evolution of the iteration error for the level set method and exact data.

It is worth noticing that the amount of available data strongly influences the quality of the reconstruction (see Figure 5). However, no matter how many voltage-current pairs one uses in the implementation of the Landweber-Kaczmarz method, it does not allow a proper determination of the p-n junction. We repeated the implementation up to $N = 45$. We observed that, after a certain number of pairs, the quality of the reconstruction does not improve any further.

In [4], a similar experiment to the one shown in Section 4 was presented. However, the authors used piecewise C^1 functions as sources (voltages) and $N = 9$. The quality of the reconstruction presented here, as well as in [4], is very poor. A possible explanation is the fact that the Landweber-Kaczmarz method does not take into consideration the assumption that the coefficient γ in (28) in the considered application is a piecewise constant function. This method tries to identify a real function defined on Ω, which is a much more complicated object than the original unknown curve (the p-n junction).

The main reason we present the implementation in Section 4 is to compare with the results obtained via the level set method. Due to the nature of the level set approach, it incorporates in a natural way the assumption that γ is piecewise constant in Ω. As a matter of fact, without this assumption the level set method could not be applied at all. The reconstruction results are much better, although we use the level set method with $N = 1$.

Acknowledgments

The work of A.L. was partially supported by the Brazilian National Research Council CNPq, grants 305823/03-5 and 474085/03-1. J.P.Z. acknowledges financial support from CNPq, grants 302161/03-1 and 474085/03-1 and from Prosul program, grant 490300. P.A.M. acknowledges support from the Austrian National Science Foundation FWF through his Wittgenstein Award 2000.

References

[1] K. Astala, L. Päivärinta, *Calderón's inverse conductivity problem in the plane,* to appear Annals of Math.

[2] L. Borcea, *Electrical impedance tomography,* Inverse Problems **18** (2002), R99–R136

[3] A. Bukhgeim, G. Uhlmann, *Recovering a potential from partial Cauchy data,* Comm. Partial Differential Equations **27** (2002), 653–668

[4] M. Burger, H.W. Engl, A. Leitão and P.A. Markowich, *On inverse problems for semiconductor equations,* Milan Journal of Mathematics, **72** (2004), 273–314

[5] M. Burger, H.W. Engl, P.A. Markowich and P. Pietra, *Identification of doping profiles in semiconductor devices,* Inverse Problems **17** (2001), 1765–1795

[6] M. Burger, H.W. Engl and P. Markowich, *Inverse doping problems for semiconductor devices,* in: T.F.Chan et al, eds., Recent Progress in Computational and Applied PDEs (Kluwer Academic/Plenum Publishers, 2002, 27–38

[7] P. Deuflhard, H.W. Engl and O. Scherzer, *A convergence analysis of iterative methods for the solution of nonlinear ill-posed problems under affinely invariant conditions,* Inverse Problems **14** (1998), 1081–1106

[8] H.W. Engl, M. Hanke and A. Neubauer, *Regularization of Inverse Problems,* Kluwer Academic Publishers, Dordrecht, 1996 (Paperback: 2000)

[9] H.W. Engl, K. Kunisch and A. Neubauer, *Convergence rates for Tikhonov regularization of nonlinear ill-posed problems,* Inverse Problems **5** (1989), 523–540

[10] H.W. Engl and O. Scherzer, *Convergence rates results for iterative methods for solving nonlinear ill-posed problems,* in D. Colton et al eds., Surveys on solution methods for inverse problems, 7–34, Springer-Verlag, Vienna, 2000

[11] Fang, W.; Ito, K. *Identifiability of semiconductor defects from LBIC images,* SIAM J. Appl. Math. **52** (1992), 1611–1626

[12] Fang, W.; Ito, K. *Reconstruction of semiconductor doping profile from laser-beam-induced current image,* SIAM J. Appl. Math. **54** (1994), 1067–1082

[13] W. Fang, K. Ito and D.A. Redfern, *Parameter identification for semiconductor diodes by LBIC imaging,* SIAM J. Appl. Math. **62** (2002), 2149–2174

[14] F. Frühauf, O. Scherzer and A. Leitão. *Analysis of regularization methods for the solution of ill–posed problems involving discontinuous operators,* SIAM J Numerical Analysis **43** (2005), 767–786

[15] P. Grisvard, *Elliptic Problems in Nonsmooth Domains,* Pittman Publishing, London, 1985

[16] A.F. Grünbaum, *Diffuse tomography: the isotropic case*, Inverse Problems **8** (1992), 409–419

[17] F.A. Grünbaum and J.P. Zubelli, *Diffuse tomography: computational aspects of the isotropic case,* Inverse Problems **8** (1992), 421–433

[18] M. Hanke, A. Neubauer and O. Scherzer, *A convergence analysis of the Landweber iteration for nonlinear ill-posed problems,* Numer. Math. **72** (1995), 21–37

[19] V. Isakov, *Inverse problems for partial differential equations,* Applied Mathematical Sciences, Springer-Verlag, New York, 1998

[20] R. Kowar and O. Scherzer, *Convergence analysis of a Landweber-Kaczmarz method for solving nonlinear ill-posed problems,* in S.I. Kabanikhin et al eds., Ill-Posed and Inverse Problems, 253–270, VSP, Boston, 2002

[21] A. Leitão and O. Scherzer. *On the relation between constraint regularization, level sets, and shape optimization,* Inverse Problems, **19** (2003), L1–L11

[22] P.A. Markowich, *The Stationary Semiconductor Device Equations,* Springer-Verlag, Vienna, 1986

[23] P.A. Markowich, C.A. Ringhofer, C. Schmeiser, *Semiconductor Equations,* Springer-Verlag, Vienna, 1990

[24] A.I. Nachman, *Global uniqueness for a two-dimensional inverse boundary value problem,* Ann. of Math. **143** (1996), 71–96

[25] O. Scherzer, *Tikhonov regularization of nonlinear ill-posed problems with applications to parameter identification in partial differential equations,* Dissertationen der Johannes-Kepler-Universität Linz, 86. Verband der Wissenschaftlichen Gesellschaften Österreichs, Vienna, 1991

[26] S. Selberherr, *Analysis and Simulation of Semiconductor Devices,* Springer-Verlag, New York, 1984

[27] B.F. Svaiter and J.P. Zubelli *Convexity for the diffuse tomography model* Inverse Problems **17** (2001), 729–738

[28] W.R. van Roosbroeck, *Theory of flow of electrons and holes in germanium and other semiconductors,* Bell Syst. Tech. J. **29** (1950), 560–607

[29] A.N. Tikhonov and V.Y. Arsenin, *Solutions of Ill-posed Problems,* John Wiley & Sons, New York, 1977